

Ab initio potential curves for the X $^2\Sigma_u^+$, A $^2\Pi_u$ and B $^2\Sigma_g^+$ states of Ca $_2^+$

Sandipan Banerjee*, John A. Montgomery, Jr., Jason N. Byrd, H. Harvey Michels, Robin Côté

Department of Physics - University of Connecticut, Storrs, CT 06269-3046, USA.

Abstract

We report *ab initio* calculations of the X $^2\Sigma_u^+$, A $^2\Pi_u$ and B $^2\Sigma_g^+$ states of the Ca $_2^+$ dimer. All electron CAS+MRCI calculations are performed for the X $^2\Sigma_u^+$ and B $^2\Sigma_g^+$ states, while valence CAS+MRCI calculations using an effective core potential are used to describe the A $^2\Pi_u$ state. A double well is found in the B $^2\Sigma_g^+$ state. Spectroscopic constants, vibrational levels, transition moments and radiative lifetimes are calculated for the most abundant isotope of calcium (^{40}Ca). The static dipole and quadrupole polarizabilities, and the leading order van der Waals coefficients are also calculated for all three states.

Keywords: Ca $_2^+$ potential curves, *ab initio* calculations, transition moments, dispersion coefficients

PACS: 31.15.-p 31.15.A- 34.20.Gj

Introduction

The presence of near degeneracies in the constituent atoms of diatomic molecules can lead to a rich structure in the resulting interaction potentials. In our recent work on the Be $_2^+$ dimer [1], we showed that the nearly degenerate 2s-2p state of beryllium leads to a complex set of low lying molecular curves, including a double minima in the lowest $^2\Sigma_g^+$ state. In this Letter, we present new computational results on the Ca $_2^+$ dimer, and demonstrate that this system also exhibits a rich manifold of low-lying molecular states. Both Be and Ca represent group 2A elements in the periodic table, with their valence electronic structures (2s) 2 and (4s) 2 , respectively. Thus, some similarities between Be $_2^+$ and Ca $_2^+$ may be expected. The calculations presented here should help guide experimental efforts on cold molecular ions.

The last few years have seen significant interest in ultracold atom-ion scattering [2, 3] in the atomic, molecular and optical physics community. The experimental realization of Bose-Einstein condensation (BEC) has led to numerous applications involving charged atomic and molecular species. The cooling and trapping [4] of charged gases at sub-kelvin (ultracold) temperatures is a topic of growing interest. The phenomena of charge transport like resonant charge transfer [5] and charge mobility [6] at ultracold temperatures have also been studied in detail. Other emerging fields of interest include ultracold plasmas [7], ultracold Rydberg gases [8] and systems involving ions in a BEC [9, 10].

In this work, we begin by describing the methods used in our calculations, and follow with a discussion of the results, which

include the potential curves of the X $^2\Sigma_u^+$, B $^2\Sigma_g^+$ and A $^2\Pi_u$ states and their spectroscopic constants. We also calculate electric dipole transition moments for the X $^2\Sigma_u^+ \leftrightarrow$ B $^2\Sigma_g^+$ and the B $^2\Sigma_g^+ \leftrightarrow$ A $^2\Pi_u$ transitions. Bound vibrational levels are computed for all the states along with Franck-Condon overlaps and radiative lifetimes for the most abundant calcium isotope (^{40}Ca 96.94%). We conclude with an analysis of long range behavior, calculation of static atomic dipole and quadrupole polarizabilities and determination of the van der Waals dispersion coefficient C_6 .

Methods

We can express the total energy of the Ca $_2^+$ dimer at any interatomic separation R as

$$E_{total} = E_{valence} + \Delta E_{core-valence} + \Delta E_{scalar-relativistic} \quad (1)$$

For calculation of the ground X $^2\Sigma_u^+$ and B $^2\Sigma_g^+$ states in Ca $_2^+$, the valence contribution to the total energy is calculated by a multi-reference configuration interaction (MRCI) method using a 18 orbital complete active space (CAS) wavefunction as a reference. The active space was chosen to include molecular counterparts of nearly degenerate 4s, 4p and 3d orbitals of Ca. The state-averaged CAS includes all doublet states correlated to Ca $^+(^2D) + \text{Ca}(^1S)$ and Ca $^+(^2S) + \text{Ca}(^1S)$ asymptotes with equal weights. We have used the augmented correlation consistent polarized valence quintuple zeta (aug-cc-pV5Z) basis set of Peterson [11, 12]. In order to assess the quality of MRCI, we do a comparison with a full CI calculation with aug-cc-pVTZ basis, and find out that the difference in total energy at the equilibrium separation of 7.3 bohrs for the X $^2\Sigma_u^+$ state of Ca $_2^+$ is 4.5 microhartrees. At large separation (1000 bohrs), this difference further reduces to 1.5 microhartrees.

*Principal corresponding author; Fax: +1 860 486 3346

Email address: banerjee@phys.uconn.edu (Sandipan Banerjee)

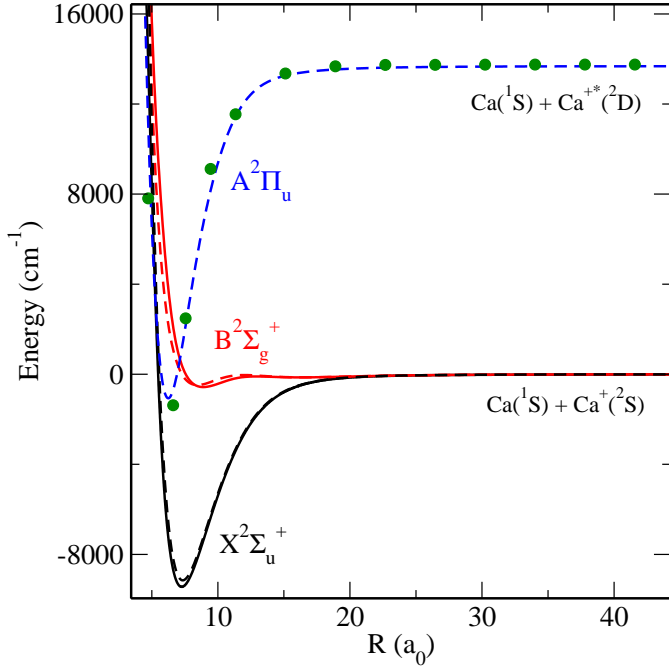


Figure 1: [COLOR ONLINE] *Ab initio* $X^2\Sigma_u^+$ (in black), $B^2\Sigma_u^+$ (in red) and $A^2\Pi_u$ (in blue) states of Ca_2^+ . Dashed lines show calculation with a pseudopotential, while solid lines show the results of an all electron correlated calculation. For the $A^2\Pi_u$ state, results of all electron MRCI calculations are shown in green \bullet . Note that a_0 is the Bohr radius (atomic unit of length).

The second term in Eq. (1), the correction from the core-valence contribution is estimated by,

$$\Delta E_{\text{core-valence}} = [E_{RIV} - E_{Val}]_R - [E_{RIV} - E_{Val}]_{R_\infty}. \quad (2)$$

The core-valence correction $\Delta E_{\text{core-valence}}$ is the difference of energies from a valence only (Ar core) and a restricted inner valence (RIV, Ne core) CCSDT calculation. For this purpose we have used the correlation consistent polarized weighted core-valence triple zeta (cc-pwCVTZ) basis set of Koput and Peterson [11]. To assess the convergence with basis set of the calculated core-valence contribution, we performed single point calculations at the equilibrium bond separation for the ground state with a larger basis set (cc-pwCVQZ). The effect of increasing the basis set from TZ to QZ changed the core-valence energy by $\sim 8 \text{ cm}^{-1}$ at the R_e of the $B^2\Sigma_g^+$ state. These results indicate that the core-valence contribution to the total energy is adequately converged with the TZ basis sets.

The last correction term $\Delta E_{\text{scalar-relativistic}}$ is the contribution from relativistic effects, which for a heavy atom like Ca is significant. This can be expressed as,

$$\Delta E_{\text{scalar-relativistic}} = [E_{\text{rel}} - E_{\text{non-rel}}]_R - [E_{\text{rel}} - E_{\text{non-rel}}]_{R_\infty}. \quad (3)$$

We have used the Douglas-Kroll version of the cc-pwCVTZ basis set from Kirk Peterson (cc-pwCVTZ-DK), and performed CCSDT calculations to estimate this correction. The magnitude of scalar relativistic correction at the equilibrium bond distance for the $B^2\Sigma_g^+$ state of the Ca_2^+ is $\sim 180 \text{ cm}^{-1}$. For Ca_2^+ , the

valence electron space contains only 3 electrons, thus the valence CCSDT is equivalent to full CI.

The calculation of the $A^2\Pi_u$ state, correlating to the Ca^+ $3d$ atomic level, is complicated by the near degeneracy with the Ca $4s4p$ atomic level. The second excited $^2\Pi_u$ state comes from an atomic asymptote of Ca $4s4p$ and Ca^+ $4s$, which lies $\sim 1500 \text{ cm}^{-1}$ above the $A^2\Pi_u$ asymptote. We find, however, that valence CAS+MRCI calculations incorrectly predict the Ca $4s4p$ and Ca^+ $4s$ asymptote to lie below the Ca $4s^2$ and Ca^+ $3d$ asymptote. The correct ordering of the atomic energy levels is obtained when core-valence correlation including double excitations of the inner valence electrons are included in the correlation treatment using the cc-pwCVQZ (or better) basis set. We expect that a balanced description of valence and core-valence interactions in the $A^2\Pi_u$ state would be obtained from a CAS(19,26)+MRCI calculation that includes molecular orbitals arising from the atomic $3s$, $3p$, $3d$, $4s$ and $4p$ orbitals. This is a much more demanding calculation than those required for the $X^2\Sigma_u^+$ and $B^2\Sigma_g^+$ states that correlate to ground states atoms. It was found that a smaller CAS(19,21)+MRCI+Q/cc-pwCVQZ (MRCI plus Davidson correction) calculation correlating the $3s3p$ inner valence electrons with a $4s3d + 4p_x$ valence reference was sufficient to obtain the correct ordering of the first and second $^2\Pi_u$ molecular states. Extending this calculation to include the entire $4p$ reference space using the cc-pwCV5Z was attempted but was too computationally demanding for our available resources. An alternative approach to the multi-reference all electron calculation is to replace the argon core of the Ca atoms with an effective-core potential (ECP) where the effects of core-valence correlation are including using a core polarization potential (CPP)[13]. This method was used with great success by Czuchaj *et al* for Ca_2 ground and excited states [14]. We have performed comparisons between the all electron calculations for the first two $^2\Sigma$ states as described above and the valence $4s4p3d$ space MRCI using the ECP+CPP and basis set of Czuchaj *et al* [14]. The agreement was found to be satisfactory for the case of the lowest Σ states as seen in Fig. 1. Additionally we have compared the $A^2\Pi_u$ state calculated using the same ECP+CPP method to the core-valence MRCI+Q/cc-pwCVQZ calculation using the $3s3p4s3d + 4p_x$ space discussed above. These two calculations agree very well, as demonstrated by Fig. 1. Because of the good agreement with the all electron calculations and the computational limitations in performing multi-reference core-valence correlation calculation, we have used the ECP+CPP method to calculate the $A^2\Pi_u$ state in this paper. We note in passing that the use of the CPP is essential; without it one does not obtain the correct ordering of the excited atomic asymptotes.

All the potential curves are also corrected for basis-set superposition error (BSSE) using the standard counterpoise technique of Boys and Bernardi [15]. The BSSE was negligible ($\sim 2 - 4 \text{ cm}^{-1}$) at the potential minima for the different curves. The MRCI valence calculations were done using the MOLPRO 2010.1 electronic structure program [16]. The core-valence

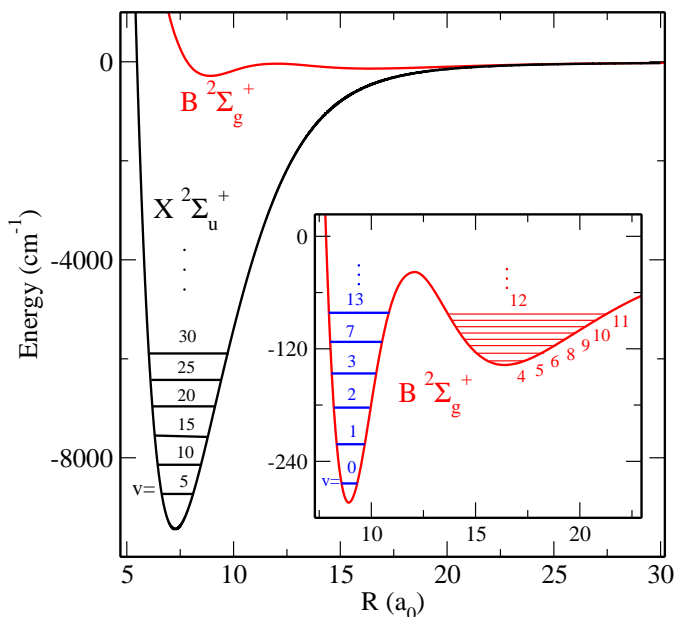


Figure 2: [COLOR ONLINE] Calculated *ab initio* potential curves of Ca_2^+ . The inset is a magnification of the double-well nature in the $\text{B } ^2\Sigma_g^+$ state (in red); lowest vibrational levels in the inner well are shown in blue thick lines and outer well in red thin lines, for ^{40}Ca .

Table 1: Calculated spectroscopic constants of Ca_2^+

State	r_e (Å)	B_e (cm^{-1})	ω_e (cm^{-1})	$\omega_e x_e$ (cm^{-1})	D_e (cm^{-1})
$\text{X } ^2\Sigma_u^+$	3.844	0.056	127.829	0.071	9440
Previous [14]	3.773		132.300		9817
Previous [23]	3.995	0.053	119.000		8388
$\text{B } ^2\Sigma_g^+$ (Inner)	4.719	0.037	41.593	0.561	284
$\text{B } ^2\Sigma_g^+$ (Outer)	8.665	0.011	8.549	3.839	137
$\text{A } ^2\Pi_u$	3.303	0.077	194.195	0.370	14746

CCSDT calculations were carried out using CFOUR (coupled-cluster techniques for computational chemistry) program [17]. The scalar relativistic corrections were done at the CCSDT level of theory using the MRCC (multi-reference coupled cluster) program [18] of M. Kállay. All of the programs were running on a Linux workstation. All calculations employed restricted open-shell (ROHF) reference wavefunctions. Le Roy's LEVEL program [19] has been used to calculate the bound vibrational levels, Franck-Condon factors and radiative lifetimes, discussed in the following section.

Results and Discussions

Potential Curves and Spectroscopic Constants

Fig. 2 shows the *ab initio* potential curves for the $\text{X } ^2\Sigma_u^+$ and $\text{B } ^2\Sigma_g^+$ states of Ca_2^+ dimer. The calculated potential energy curves are corrected for the effects of basis set superposition

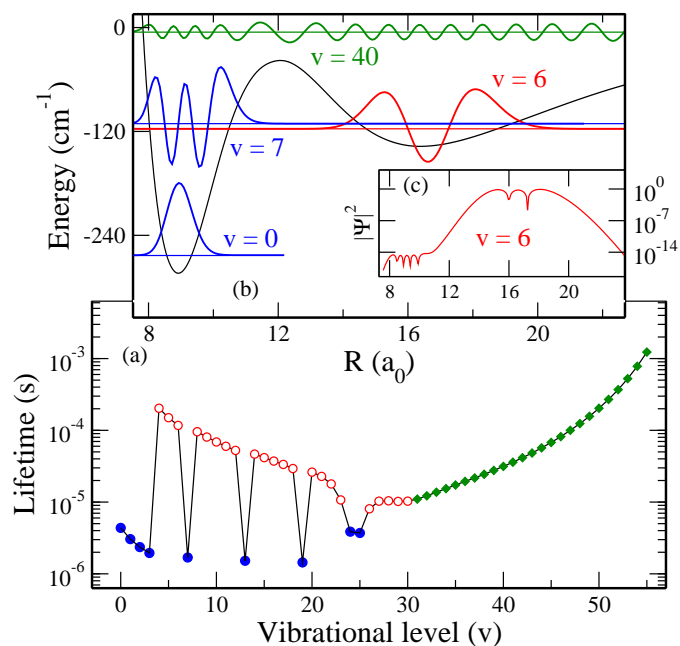


Figure 3: [COLOR ONLINE] (a) Calculated radiative lifetimes of bound levels of $^{40}\text{Ca}_2^+$ in the $\text{B } ^2\Sigma_g^+$ state, on a log-scale. The shorter lifetimes (blue \bullet) correspond to bound levels localized in the inner well, the longer lifetimes (red \circ) to levels localized in outer well, and the increasingly longer lifetimes (green \blacklozenge) to levels spread over both wells. (b) show examples of each cases: $v=0$ and 7 in the inner well, $v=6$ in the outer well, and $v=40$ in both. (c) depicts $|\psi|^2$ of $v=6$ on a log-scale; showing that the amplitude in the inner well is extremely small. The reverse is true for $v=7$ and so on.

error by the counterpoise method of Boys and Bernardi[15]. Fig.1 shows the $\text{A } ^2\Pi_u$ state. We have used a standard Dunham analysis [20] to calculate the spectroscopic constants (Table 1). We calculate bound vibrational levels for the $\text{X } ^2\Sigma_u^+$, $\text{B } ^2\Sigma_g^+$ and $\text{A } ^2\Pi_u$ state for the $^{40}\text{Ca}_2^+$ dimer.

Unfortunately there are no experimental spectroscopic data for the ground or excited states of the Ca_2^+ dimer. There are, however, some previous theoretical studies of Ca_2 [14, 21] and Ca_2^+ [14, 22, 23], and a comparison to the results for the $\text{X } ^2\Sigma_u^+$ state is listed in Table 1. No spectroscopic constants have been reported for the most recent calculation by Sullivan *et al.* [22]. Another approach for calculating interaction energies in alkaline earth elements, is using symmetry-adapted perturbation theory (SAPT), which has been demonstrated earlier by Patkowski *et al.*[24]. The $\text{B } ^2\Sigma_g^+$ state has a double well similar to that found in our recent Be_2^+ calculations [1]. Both of these wells support bound vibrational states. This double-well nature of the $\text{B } ^2\Sigma_g^+$ state is most likely caused by perturbations from an excited $^2\Sigma_g^+$ state.

We have calculated radiative lifetimes (see Fig.3) for bound vibrational levels in both the inner and outer wells of the $\text{B } ^2\Sigma_g^+$ state. Since these wells are separated by a large barrier, the wavefunction of the lower vibrational levels can be strongly localized in either wells. The localization of the vibrational wavefunctions can be attributed to the asymmetry of the double well

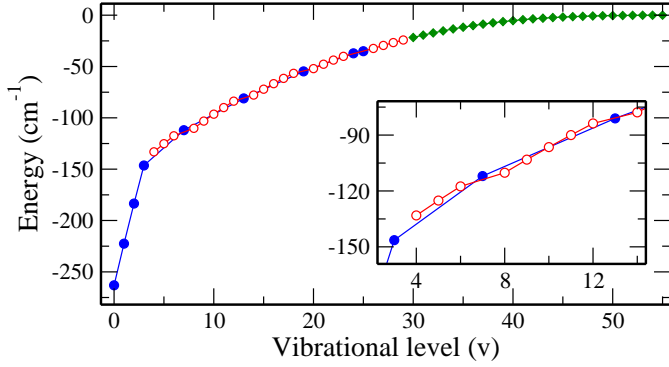


Figure 4: [COLOR ONLINE] Energies of bound levels of B $^2\Sigma_g^+$ state in $^{40}\text{Ca}_2^+$ using the same convention as in Fig.3. The inset magnifies the difference in slopes of levels localized in the inner well (shown in blue) from the ones in the outer well (shown in red).

(see Fig.2) and disappears for levels above the barrier. The behavior of the radiative lifetimes exhibits 3 distinct regimes, one where the wavefunction is mainly localized in the inner well (in blue), one where it is localized in the outer well (in red), and the last being the region (in green) in which the wavefunction spreads over both wells, resulting in poor Franck-Condon overlap with the ground X $^2\Sigma_u^+$ state and hence longer lifetimes. The inset shows the square of the amplitude of wavefunction in $v=6$, of B $^2\Sigma_g^+$ state in a logarithmic plot as a demonstration that the amplitude is negligible inside the inner well but still finite, preserving the correct number of nodes for that level. Fig.4 shows a plot of the energies of all bound vibrational levels in the B $^2\Sigma_g^+$ state of $^{40}\text{Ca}_2^+$. The localization effect of wavefunctions discussed above is also exhibited in this plot; the density of levels in the more extended outer well is larger than in the inner well, leading to different energy slopes. The inset of Fig.4 exemplifies this point.

Electronic dipole transition moments

For homonuclear molecules like Ca_2^+ , there is no permanent dipole moment. However there are transitions between different electronic states which are dipole allowed. We calculate two transition moments, one of them couples the ground X $^2\Sigma_u^+$ and B $^2\Sigma_g^+$ states, and the other one couples the B $^2\Sigma_g^+$ state to the excited A $^2\Pi_u$ state. To compute these transition moments, we use a complete active space self consistent field (CASSCF) wavefunction as a reference for performing multi-reference configuration interaction (MRCI) calculations. The core-valence contribution to the electronic transition moment is found to be negligible and hence omitted in the present calculations. The calculation of the transition moment coupling the B $^2\Sigma_g^+$ state to the excited A $^2\Pi_u$ state was done with the ECP+CPP valence CAS+MRCI method.

The electronic dipole transition moment (in atomic units) is given by,

$$\mu_{12}(R) = \langle 2 | z | 1 \rangle, \quad (4)$$

where $|1\rangle$ and $|2\rangle$ are the electronic wave functions corresponding to the pair of states X $^2\Sigma_u^+ \leftrightarrow$ B $^2\Sigma_g^+$ or B $^2\Sigma_g^+ \leftrightarrow$ A $^2\Pi_u$,

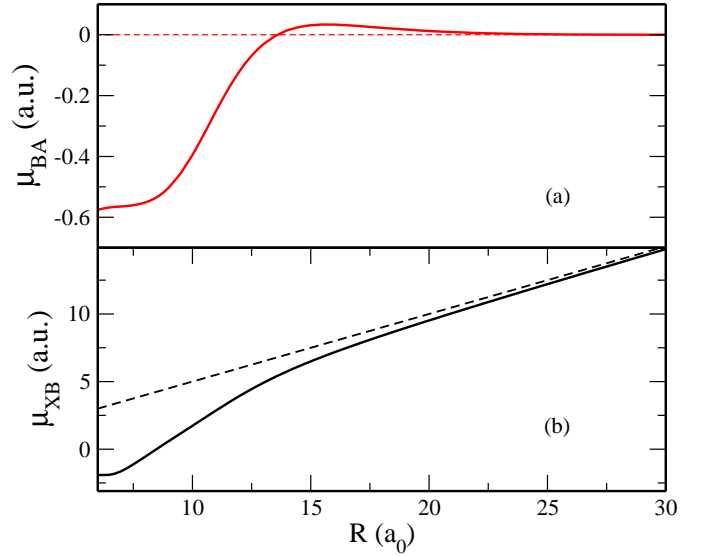


Figure 5: [COLOR ONLINE] Computed electronic dipole transition moment, μ_{BA} coupling the B $^2\Sigma_g^+$ to the A $^2\Pi_u$ state shown in red (a) and μ_{XB} coupling the X $^2\Sigma_u^+$ to the B $^2\Sigma_g^+$ state shown in black (b). The dashed line $R/2$ in (b), corresponds to the classical dipole behavior.

when the two Ca nuclei are separated by the distance R .

Fig. 5(a) shows the electronic transition dipole moment coupling the B $^2\Sigma_g^+$ and the A $^2\Pi_u$ state. The transition moment goes to zero asymptotically. Fig. 5(b) shows a plot of the computed electronic dipole transition moment between the B $^2\Sigma_g^+$ and the X $^2\Sigma_u^+$ ground states of Ca_2^+ . The transition moment μ_{XB} coupling the X $^2\Sigma_u^+$ and B $^2\Sigma_g^+$ states asymptotically follows the classical dipole behavior, $\mu_{XB} \sim R/2$ [25, 26]; we observe this behavior in the calculated curve of Fig. 5(b). We note that although the transition moment grows linearly with R , the probability of spontaneous transition will tend to zero since it is proportional to ν_{XB}^3 , which vanishes exponentially as $R \rightarrow \infty$.

Polarizabilities and dispersion coefficients

For large internuclear separations, the long-range form of the intermolecular potential can be written as

$$V_{LR}(R) = V_\infty - \sum_n \frac{C_n}{R^n}, \quad (5)$$

which, for the molecular ion Ca_2^+ , can be approximated by

$$V_{LR}(R) \sim V_\infty - \frac{C_4}{R^4} - \frac{C_6}{R^6}, \quad (6)$$

where V_∞ is the energy of the atomic asymptote; $C_4 = \alpha_d/2$, α_d is the static dipole polarizability, $C_6 = (\alpha_q/2 + c_6)$, α_q is the quadrupole polarizability and c_6 the Van der Waals dispersion coefficient. In the expression for long range energy we have ignored the exchange energy contribution E_{exch} which is very small. Also we have truncated the series at powers of R^{-6} , not

Table 2: The static atomic dipole, quadrupole polarizabilities and dispersion coefficient for $X^2\Sigma_u^+$, $B^2\Sigma_g^+$ and $A^2\Pi_u$ states of Ca_2^+ . All values are in atomic units. The square brackets indicate powers of ten.

Molecular State	Dipole polarizability (α_d)	Quadrupole polarizability (α_q)	C_4 ($=\alpha_d/2$)	Dispersion coefficient (c_6)	C_6 ($=\alpha_q/2+c_6$)
$X^2\Sigma_u^+$, $B^2\Sigma_g^+$	1.606[2]	3.073[3]	8.032[1]	1.081[3]	2.618[3]
Previous [27]	1.571[2]	3.081[3]			
Previous [28]				1.085[3]	
$A^2\Pi_u$	1.606[2]	3.073[3]	8.032[1]	4.950[2]	2.031[3]
Previous [30]					

including contributions from R^{-8} and R^{-10} order coefficients.

We have performed finite-field CCSD(T) calculations with the aug-cc-pV5Z basis set using MOLPRO to estimate the values of the static atomic dipole and quadrupole polarizabilities. We obtain $\alpha_d = 160.64$ a.u. and $\alpha_q = 3073.39$ a.u which are both in good agreement with a previous result [27] of 157.1 a.u. and 3081 a.u. respectively. The values of static dipole and quadrupole polarizability do not change for the excited $A^2\Pi_u$ state, since it comes from an atomic asymptote in which the Ca ion is in an excited 2D state whereas the Ca atom is in ground 1S state (see Fig.1). Using a numerical fit, as described by Banerjee *et al.* [1], we were able to extract the value of the dispersion coefficient c_6 for all the states. The value of dispersion coefficient for ground states are in good agreement with unpublished results of Mitroy [28], which are done by the methods used by Mitroy and Zhang [29, 30] for Ca and Ca^+ . Table [2] lists the values of polarizabilities and dispersion coefficient for $X^2\Sigma_u^+$, $B^2\Sigma_g^+$ and $A^2\Pi_u$ states of the Ca_2^+ dimer.

Concluding Remarks

Ab initio calculations have been performed on the $X^2\Sigma_u^+$, $B^2\Sigma_g^+$ and $A^2\Pi_u$ states of the Ca_2^+ dimer. The calculations were computationally challenging as well as expensive because of the near degeneracy of the 4s-4p-3d orbitals in Ca. Since the $B^2\Sigma_g^+$ state has a double well, one of them being near 16.5 a_0 , it was necessary to include diffuse functions in the basis sets to describe the well accurately. For calculating the ground $X^2\Sigma_u^+$ and $B^2\Sigma_g^+$ states, large augmented correlation consistent basis sets of Koput and Peterson [11] were thus chosen and the results were also corrected for basis-set superposition error. We have also corrected our valence only MRCI results for core-valence and scalar relativistic effects using CCSDT calculations with both restricted inner valence and frozen core using Peterson’s cc-pwCVTZ basis set. The $A^2\Pi_u$ state was calculated with an ECP + CPP approach similar to the previous calculations of Czuchaj *et al.*[14]. Numerical values of the calculated potential energies are available from the authors upon request.

Due to lack of experimental data, we were unable to compare our theoretical values for dissociation energies or spectroscopic

constants. However there are some previous theoretical results for spectroscopic constants for the $X^2\Sigma_u^+$ ground state of Ca_2^+ [14, 23]. These values compare well with our calculated results (see Table 1).

The calculation of radiative lifetimes of $^{40}\text{Ca}_2^+$ in the $B^2\Sigma_g^+$ state, reflects the wavefunction localization in either of the double wells. This causes the levels in the inner well to have a shorter lifetime ($\sim \mu\text{s}$), whereas the ones in the outer well have much longer lifetimes ($\sim \text{ms}$). These vibrational levels in the $B^2\Sigma_g^+$ state should generate interest for experiments in ultracold atomic and molecular physics, where these long lived molecular ions could be observed. We believe there are new prospects in both theory and experiments for atom-ion collisions, resonant charge transfer and quantum information storage using Ca_2^+ molecular ions.

Acknowledgements

This work has been supported in part by the U.S. Department of Energy Office of Basic Sciences. We would like to thank Kirk Peterson for sharing his augmented functions for the correlation consistent basis sets and Jim Mitroy for sharing his calculated dispersion coefficients. We are extremely grateful to the referees for their very perceptive comments on this manuscript.

Primary Author Information

Dr. S. Banerjee is presently a Research Engineer at Intel Corporation. His other publications can be found here [31–49].

References

- [1] S. Banerjee, J. N. Byrd, R. Côté, H. H. Michels, J. A. Montgomery Jr., Chem. Phys. Lett. 496 (2010) 208.
- [2] P. Zhang, A. Dalgarno, R. Côté, E. Bodo, Phys. Chem. Chem. Phys. (2011) 1.
- [3] P. Zhang, A. Dalgarno, R. Côté, Phys. Rev. A 80 (2009) 030703.
- [4] J. Weiner, V. Bagnato, S. Zilio, P. Julienne, Rev. Mod. Phys. 71 (1999) 1.
- [5] R. Côté, A. Dalgarno, Phys. Rev. A 62 (2000) 012709.
- [6] R. Côté, Phys. Rev. Lett. 85 (2000) 5316.
- [7] T. C. Killian, S. Kulin, S. D. Bergeson, L. A. Orozco, C. Orzel, S. L. Rolston, Phys. Rev. Lett. 83 (1999) 4776.

- [8] W. R. Anderson, J. R. Veale, T. F. Gallagher, *Phys. Rev. Lett.* 80 (1998) 249.
- [9] R. Côté, V. Kharchenko, M. D. Lukin, *Phys. Rev. Lett.* 89 (2002) 093001.
- [10] D. Ciampini, M. Anderlini, J. H. Müller, F. Fuso, O. Morsch, J. W. Thomsen, E. Arimondo, *Phys. Rev. A* 66 (2002) 043409.
- [11] J. Koput, K. A. Peterson, *J. Phys. Chem. A* 106 (2002) 9595.
- [12] K. Peterson, private communication, 2010.
- [13] P. Fuentealba, L. von Szentpály, H. Preuss, H. Stoll, *J Phys. B* 18 (1985) 1287.
- [14] E. Czuchaj, M. Krosnicki, H. Stoll, *Theo. Chem. Accts.* 110 (2003) 28.
- [15] S. F. Boys, F. Bernardi, *Mol. Phys.* 19 (1970) 553.
- [16] H.-J. Werner, P. J. Knowles, R. Lindh, F. R. Manby, M. Schütz, et al., MOLPRO, version 2010.1, a package of ab initio programs, see <http://www.molpro.net>, 2010.
- [17] J. Stanton, J. Gauss, M. Harding, P. Szalay, et al., CFOUR, Coupled-Cluster techniques for Computational Chemistry, see <http://www.cfour.de>, 2010.
- [18] M. Kállay, P. R. Surján, *J. Chem. Phys.* 115 (2001) 2945.
- [19] R. J. Le Roy, Univ. of Waterloo Chem. Phys. Research Report CP-663 (2007).
- [20] J. L. Dunham, *Phys. Rev.* 41 (1932) 721.
- [21] B. Bussery-Honvault, R. Moszynski, *Mol. Phys.* 104 (2006) 2387.
- [22] S. T. Sullivan, W. G. Rellergert, S. Kotochigova, K. Chen, S. J. Schowalter, E. R. Hudson, *Phys. Chem. Chem. Phys.* 13 (2011) 18859.
- [23] B. Liu, R. E. Olson, *Phys. Rev. A* 18 (1978) 2498.
- [24] K. Patkowski, R. Podeszwa, K. Szalewicz, *J. Phys. Chem. A* 111 (2007) 12822.
- [25] W. J. Stevens, M. Gardner, A. Karo, P. Julienne, *J. Chem. Phys.* 67 (1977) 2860.
- [26] H. H. Michels, R. H. Hobbs, L. A. Wright, *J. Chem. Phys.* 71 (1979) 5053.
- [27] S. Porsev, A. Derevianko, *JETP* 102 (2006) 195.
- [28] J. Mitroy, private communication, 2010.
- [29] J. Mitroy, J.-Y. Zhang, *J. Chem. Phys.* 128 (2008) 134305.
- [30] J. Mitroy, J. Y. Zhang, *Eu. Phys. J. D* 46 (2008) 415.
- [31] D. Shu, S. Banerjee, J. A. Montgomery Jr, *Bulletin of the American Physical Society* 59.
- [32] W. Smith, D. Goodman, I. Sivarajah, J. Wells, S. Banerjee, R. Côté, H. Michels, J. Montgomery Jr, F. Narducci, *Applied Physics B* 114 (1-2) (2014) 75–80.
- [33] S. Banerjee, J. A. Montgomery, J. A. Gascon, Scalable quantum chemical approaches for the study of protected gold nano-clusters, in: ABSTRACTS OF PAPERS OF THE AMERICAN CHEMICAL SOCIETY, vol. 244, AMER CHEMICAL SOC, 2012.
- [34] M. N. Dailey, S. Banerjee, J. A. Gascon, Force field development for thiolated gold nanoclusters, in: ABSTRACTS OF PAPERS OF THE AMERICAN CHEMICAL SOCIETY, vol. 245, AMER CHEMICAL SOC, 2013.
- [35] S. Banerjee .
- [36] S. Banerjee, J. Montgomery, *Bulletin of the American Physical Society* 58.
- [37] D. Valente, S. Banerjee, *Bulletin of the American Physical Society* 58.
- [38] D. Shu, S. Banerjee, J. Montgomery, *Bulletin of the American Physical Society* 58.
- [39] S. Banerjee, J. Montgomery, R. Côté, Calculation of ab initio potential curves for ground and low lying excited states of heteronuclear alkaline earth dimers BeCa^+ , BeMg^+ and MgCa^+ , in: APS Division of Atomic, Molecular and Optical Physics Meeting Abstracts, vol. 1, 7002, 2012.
- [40] S. Banerjee, J. Byrd, R. Côté, H. Michels, J. Montgomery, Ab initio potential curves for the ground states of Ca^{2+} : Existence of a double minimum in the $A^2 \sigma_{g^+}$ state, in: APS Division of Atomic, Molecular and Optical Physics Meeting Abstracts, vol. 1, 5004, 2011.
- [41] S. Banerjee, J. N. Byrd, R. Côté, H. H. Michels, J. A. Montgomery Jr .
- [42] S. Banerjee, J. Montgomery, J. Byrd, H. Michels, R. Côté, Calculation of potential curves for the $X^2 \sigma_{u^+}$ and $A^2 \sigma_{g^+}$ states of Be^{2+} : Existence of a double minimum, in: APS Division of Atomic, Molecular and Optical Physics Meeting Abstracts, vol. 1, 2006, 2010.
- [43] S. Banerjee, M. Gacesa, R. Côté, Forming ultracold LiK molecules from Li-K mixtures, in: APS Division of Atomic, Molecular and Optical Physics Meeting Abstracts, vol. 1, 1095, 2009.
- [44] S. Banerjee, J. A. Montgomery Jr, J. N. Byrd, H. H. Michels, R. Côté, *Chemical Physics Letters* 542 (2012) 138–142.
- [45] S. Banerjee, J. Byrd, R. Côté, H. Michels, J. Montgomery, Formation of Be^{2+} molecules in the metastable $B^2 \sigma_{g^+}$ state by ultracold photoassociation, in: APS Division of Atomic, Molecular and Optical Physics Meeting Abstracts, vol. 1, 1029, 2011.
- [46] S. Banerjee, J. A. Montgomery Jr, J. A. Gascón, *Journal of Materials Science* 47 (21) (2012) 7686–7692.
- [47] S. Banerjee, J. Byrd, H. Michels, J. Montgomery, *Bulletin of the American Physical Society* 56.
- [48] S. Banerjee, J. Montgomery, *Bulletin of the American Physical Society* 57.
- [49] S. Banerjee, J. N. Byrd, R. Côté, H. Harvey Michels, J. A. Montgomery Jr, *Chemical Physics Letters* 496 (1) (2010) 208–211.